

**Expression Profiling of Differentially  
Expressed Genes Under Stress  
Conditions and FLC1 Modulation in  
*Cryptococcus neoformans***

Diego Cesar Villa Almeyda

Master of Science

July, 2025

School of Mathematics  
The University of Edinburgh

Dissertation Presented for the Degree of MSc in Statistics with Data Science

# Table of contents

<b>Own work declaration</b>	<b>3</b>
<b>Executive summary</b>	<b>4</b>
<b>1 Introduction</b>	<b>5</b>
<b>2 Methods</b>	<b>6</b>
2.1 Experimental design and data . . . . .	6
2.2 Pre-filtering . . . . .	6
2.3 Normalisation and transformation . . . . .	7
2.4 Exploratory analysis . . . . .	7
2.5 Differential expression analysis . . . . .	8
2.6 Software . . . . .	10
<b>3 Results</b>	<b>11</b>
3.1 Pre-processing . . . . .	11
3.2 Quality assessment and exploratory analysis . . . . .	11
3.3 Differential expression analysis . . . . .	15
3.4 Gene expression profiles . . . . .	16
3.5 Gene prioritization . . . . .	20
<b>4 Conclusions</b>	<b>22</b>
<b>References</b>	<b>23</b>
<b>Appendix</b>	<b>25</b>
Word count . . . . .	25
Supplementary figures . . . . .	25

# Own work declaration

**Name:** Diego Cesar Villa Almeyda

**Matriculation Number:** S2750743

**Title of work:** Differential Gene Expression in *Cryptococcus neoformans* Cell Wall Stress Response

I confirm that all this work is my own except where indicated, and that I have:

- Clearly referenced/listed all sources as appropriate.
- Referenced and put in inverted commas all quoted text (from books, web, etc)
- Given the sources of all pictures, data etc. that are not my own.
- Not made any use of the report(s) or essay(s) of any other student(s) either past or present.
- Not sought or used the help of any external professional academic agencies for the work.
- Acknowledged in appropriate places any help that I have received from others (e.g. fellow students, technicians, statisticians, external sources).
- Complied with any other plagiarism criteria specified in the Course handbook.

I understand that any false claim for this work will be penalised in accordance with the University regulations (<https://teaching.maths.ed.ac.uk/main/msc-students/msc-programmes/statistics/data-science/assessment/academic-misconduct>)[<https://teaching.maths.ed.ac.uk/main/msc-students/msc-programmes/statistics/data-science/assessment/academic-misconduct>].

Signature:



Date: 1st July 2025

# Executive summary

This report analyses RNA-seq data from an experiment designed to understand how *Cryptococcus neoformans* responds to cell wall stress under varying genetic and environmental conditions, with a focus on the FLC1 gene, a candidate antifungal drug target. Cells from wild-type and FLC1 $\Delta$  strains were grown under combinations of temperature (30°C or 37°C) and growth media (YPD, with or without CFW and/or EGTA), simulating stress conditions.

The analysis confirmed strong biological replicate consistency of the experimental data and revealed that strain background shaped the response to stress: FLC1 $\Delta$  cells displayed more pronounced expression changes, particularly in response to CFW and at higher temperatures. Key driver genes of this variation included FLC1 gene itself (CNAG\_04283), as well as CNAG\_01653, CNAG\_04891, and CNAG\_00588.

Differential expression analysis identified over 3,400 genes (52.4%) with significant changes related to the interaction of the experimental factors, especially when contrasting the FLC1 $\Delta$  strain under compound stress (CFW + EGTA at 37°C) with the wild-type strain under basal medium at 37°C, where most were downregulated. One gene, CNAG\_06576, showed consistent high significance and condition-specific regulation. Clustering the top 500 most informative DE genes revealed four major expression patterns, primarily driven by strain and stress condition, with one cluster reflecting stress-induced repression in the mutant FLC1 $\Delta$  strain.

The findings suggest FLC1 plays a key role in mediating the transcriptional stress response. A ranked list of the top 100 DE genes is provided for future functional characterisation. While robust, the results are based on a single DE method (**DESeq2**), and could be further validated using complementary statistical methods.

# 1 Introduction

*Cryptococcus neoformans* is a globally distributed fungal pathogen responsible for hundreds of thousands of deaths annually, mainly affecting immunocompromised individuals (1). Treatment options are limited and increasingly compromised by drug resistance, with all major antifungal classes (polyenes, azoles, and pyrimidine analogues) facing challenges related to toxicity and reduced efficacy. This high disease burden, coupled with rising antifungal resistance, highlights an urgent need for novel therapeutic strategies.

Recent studies have identified the FLC1 protein as a critical factor in *C. neoformans* stress response and virulence (2). Because FLC1 homologues are present in other fungal pathogens but poorly conserved in humans, it presents a promising drug target that could enable broad-spectrum antifungal therapies with reduced host toxicity. Motivated by this, the present report analyses transcriptomic data from an experiment by Rachel Murray (Wallace Lab, University of Edinburgh) exploring fungal responses to cell wall stressors—calcofluor white (CFW), EGTA (a calcium chelator), and deletion of FLC1, which is implicated in calcium import. Preliminary observations showed that FLC1 deletion causes abnormal cell wall morphology and lethality at 37°C, effects that EGTA can suppress. This analysis aims to uncover the gene expression changes underlying these phenotypes and provide a statistical foundation for further biological insights.

RNA sequencing (RNA-Seq) is a high-throughput technology that enables accurate, genome-wide profiling of gene expression and transcript isoforms at single-base resolution (3). In the described experiment, RNA-Seq measured transcript abundance across thousands of genes after a 3-hour incubation under varying environmental (growth media and temperature) and genetic (presence or deletion of FLC1) conditions.

Our analysis of this RNA-Seq data had three main goals: (i) assess replicate quality and explore broad expression patterns across samples; (ii) identify genes differentially expressed in response to environmental or genetic changes; and (iii) characterise distinct expression patterns within these differentially expressed genes. These efforts provide robust statistical evidence to guide further biological interpretation and prioritise candidate genes for functional studies of cell wall stress mechanisms in *C. neoformans*.

## 2 Methods

### 2.1 Experimental design and data

The study involved culturing cells from both the wild-type (WT, FLC1 gene present) and FLC1 $\Delta$  (FL, FLC1 gene absent) strains under various environmental conditions. Cells were grown in four different growth medium: YPD (Y), YPD with CFW (YC), YPD with EGTA (YE), and YPD with both CFW and EGTA (YCE), all at 37°C to induce stress. Additionally, both strains were grown under baseline conditions in standard YPD at 30°C. In total, 10 distinct experimental conditions were tested (5 environmental conditions  $\times$  2 strains), each with 3 biological replicates, resulting in 30 samples.

Table 2.1 presents the experimental design along with the sample labels for each condition. The 10 experimental conditions are labeled by combining the levels of the three experimental factors: strain, temperature, and growth media, in that order. For example, the condition involving the wild-type strain grown in YCE medium at 37°C is labeled WT-37-YCE, while the corresponding condition for the FLC1 $\Delta$  strain is labeled FL-37-YCE.

The primary output of the experiment was a raw count matrix containing RNA abundance measurements for 6795 genes across 30 samples, resulting in a 6795  $\times$  30 matrix. Each entry in the matrix represents the number of sequencing reads mapped to a specific gene in a given sample.

### 2.2 Pre-filtering

Genes with consistently low or zero counts across samples are unlikely to be biologically active and are typically excluded before DE analysis. This pre-filtering step is justified because genes must surpass a minimal expression threshold to produce functional proteins or exert biological effects (4), and low counts often reflect sampling noise rather than true signal (5).

Filtering also improves statistical power. Since DE analysis tests each gene for expression differences between conditions, it involves multiple hypothesis testing, typically corrected via FDR adjustment. These corrections reduce power, especially when many genes are

**Table 2.1:** Overview of the experimental design showing the combinations of temperature and growth media (environmental conditions) used to grow cells of the WT and FLC1 $\Delta$  (FL) strains. Each cell lists the replicate sample labels (S1–S30) corresponding to each unique experimental condition.

Strain	Environmental conditions				
	30°C		37°C		
	Y	YC	YE	YCE	
WT	S1, S2, S3	S4, S5, S6	S7, S8, S9	S10, S11, S12	S13, S14, S15
FL	S16, S17, S18	S19, S20, S21	S22, S23, S24	S25, S26, S27	S28, S29, S30

tested but few are truly DE (6). Removing low-expression genes reduces the number of tests, making FDR correction less stringent and increasing the likelihood of detecting true positives (5,6).

Although the software used for differential expression (DE) analysis includes an internal filtering routine (see Section 2.5), additional pre-filtering was applied using an empirical method implemented in the R package `edgeR` (7), as described in (4). This method retains genes whose counts-per-million (CPM) exceed a specified threshold  $k$  in at least  $n$  samples. The CPM for each gene in a sample is calculated by dividing the raw read count by the total number of reads (i.e., the library size) in that sample and scaling by one million.

To determine the CPM threshold  $k$ , the user specifies a minimum raw count that a gene must meet in  $n$  samples, and the software computes the corresponding CPM based on the smallest library size. For this study, we required a minimum count of 10 in at least 3 samples, corresponding to the number of replicates per condition. The original, unfiltered count matrix was retained to replicate the DE analysis and compare results.

## 2.3 Normalisation and transformation

In RNA-seq experiments, raw read counts are influenced by both gene expression and technical factors, such as library size, gene length, and GC content, making them not directly comparable across samples or genes (8,9). Between-sample variation, mainly due to differences in library size, is commonly corrected using normalisation methods.

While total count normalisation (e.g., CPM) adjusts for library size, it can be biased by a few highly expressed genes, potentially distorting the expression estimates of others and introducing artefactual differences (8). More robust approaches like TMM have been proposed (10). In this study, we used the `DESeq2` median-of-ratios method to estimate sample-specific size factors (11,12), and CPM was also applied for comparison. Within-sample normalisation (e.g., for gene length or GC content) was not performed, following the project advisor's recommendation.

RNA-seq data visualisation and multivariate analyses like clustering or PCA are sensitive to heteroskedasticity, where genes with higher expression tend to show greater variance. This can allow highly expressed genes to dominate the analysis and obscure biological signals (12). Variance-stabilising transformations (VSTs) are often used to place genes on a comparable scale (13).

Log transformation is a common approach but tends to exaggerate variability in low-count genes, where noise can dominate (12). In this study, we applied the regularised log (rlog) and VST methods implemented in `DESeq2` (11,12), both applied after `DESeq2` normalisation. For comparison, we also used a base-2 log transformation on CPM-normalised counts, with a prior count of 2 to avoid undefined values.

Transformations were assessed using mean–SD plots for gene-wise variance and boxplots of sample expression profiles to evaluate the extent of variance stabilisation.

## 2.4 Exploratory analysis

An important early step in RNA-seq analysis is assessing the quality and consistency of biological replicates. Ideally, replicates under the same condition should show similar

expression profiles after normalisation and transformation. To evaluate this, we used principal component analysis (PCA) to project samples into a lower-dimensional space and examine whether replicates cluster together. PCA decomposes the expression matrix into uncorrelated components ordered by the variance they explain, offering a visual summary of sample similarity. We applied Horn's parallel analysis to determine how many components to retain, comparing observed eigenvalues to those from randomly generated data and keeping components that exceeded the simulated average (14). This analysis was performed on three transformed datasets: log-transformed CPM, rlog-transformed counts, and VST-transformed counts, as described in Section 2.3.

To visualise sample structure and identify genes contributing to variation, we generated PCA biplots showing the samples along with the five genes most strongly correlated with each principal component, based on their loadings. Loading plots displaying the top 10 of genes by absolute loading value were also produced. To explore the relationship between experimental conditions and the principal components, we conducted ANOVA tests on the component scores, using each experimental factor as a grouping variable. All PCA analyses were performed using the top 10% most variable genes, which are more likely to reflect meaningful biological signals, while low-variance genes were excluded as typically uninformative.

## 2.5 Differential expression analysis

The DE analysis approach used in this study follows the methodology implemented in the `DESeq2` package. The core idea is to model the raw counts for each gene using a negative binomial (NB) distribution, where the logarithm of the normalised mean is modeled as a linear combination of coefficients corresponding to contrasts of experimental conditions. Hypothesis testing is then performed on these coefficients to assess whether the corresponding contrasts result in statistically significant differential expression for a given gene. In the remainder of this section, we briefly outline the key features of this modeling framework, as described in (12).

Let  $c_{ij}$  denote the observed raw count for gene  $i$  in sample  $j$ . We assume that  $c_{ij}$  has a NB distribution with mean  $\mu_{ij}$  and gene-specific dispersion parameter  $\alpha_i$ ; that is,  $c_{ij} \sim \mathcal{NB}(\mu_{ij}, \alpha_i)$ . The mean  $\mu_{ij}$  is modelled as the product of a sample-specific size factor  $s_j$  and a normalised expression level  $q_{ij}$ , such that  $\mu_{ij} = s_j q_{ij}$ . The size factor  $s_j$  is estimated using the median-of-ratios method, as mentioned in Section 2.3. Finally, the dispersion parameter is used to model the variance of the counts via  $\text{var}(c_{ij}) = \mu_{ij} + \alpha_i \mu_{ij}^2$ .

The log-transformation of the normalised expression level,  $q_{ij}$ , is modelled in this study as

$$\log(q_{ij}) = \beta_{i0} + \beta_{i1}x_j^{(\text{FL})} + \beta_{i2}x_j^{(\text{YC})} + \beta_{i3}x_j^{(\text{YE})} + \beta_{i4}x_j^{(\text{YCE})} + \beta_{i5}x_j^{(30)} + \beta_{i6}x_j^{(\text{FL})}x_j^{(\text{YC})} + \beta_{i7}x_j^{(\text{FL})}x_j^{(\text{YE})} + \beta_{i8}x_j^{(\text{FL})}x_j^{(\text{YCE})} + \beta_{i9}x_j^{(\text{FL})}x_j^{(30)}, \quad (2.1)$$

where the intercept term  $\beta_{i0}$  denotes the baseline expression level of gene  $i$  under the reference condition. The coefficients  $\beta_{i1}$  to  $\beta_{i5}$  represent the main effects of the experimental factors:  $x_j^{(\text{FL})}$  is an indicator variable for the FLC1 $\Delta$  strain, with the WT strain serving as the reference level;  $x_j^{(\text{YC})}$ ,  $x_j^{(\text{YE})}$ , and  $x_j^{(\text{YCE})}$  are indicators for the different media conditions, with Y as the reference level; and  $x_j^{(30)}$  indicates the 30°C temperature condition, with 37°C as reference. Together, this implies that the reference experimental

condition is WT-37-Y. The interaction terms  $\beta_{i6}$  to  $\beta_{i9}$  model how the effects of media and temperature differ under the presence or absence of the FLC1 gene. No interaction between media and temperature was included, as these factors are not fully crossed in the experimental design.

Accurate estimation of gene-specific dispersion parameters ( $\alpha_i$ ) is essential for reliable differential expression analysis. However, in experiments with small sample sizes—such as this one—maximum likelihood estimates (MLE) of dispersion can be highly variable and compromise significance testing (12). To address this, **DESeq2** applies an empirical Bayes shrinkage approach that pulls dispersion estimates toward a trend based on mean expression. This trend is derived from gene-wise estimates and modelled using a parametric regression, with final dispersion values obtained as maximum a posteriori (MAP) estimates under a log-normal prior. In cases where the gene-wise estimate notably exceeds the trend, **DESeq2** retains the original estimate to avoid underestimating true variance and inflating false positives.

The log-fold change (LFC), typically expressed on a  $\log_2$  scale, represents the change in gene expression between two conditions and corresponds to the model coefficients in Equation 2.1, estimated via MLE using the shrunken dispersion values. However, MLE-derived LFCs can be highly variable, especially for low-count genes. To improve their stability and interpretability, **DESeq2** applies an empirical Bayes shrinkage procedure introduced by (15) and implemented in the `apeglm` package. This approach uses a heavy-tailed Cauchy prior, with the prior scale adaptively estimated from the data, and produces MAP estimates that combine the negative binomial likelihood with the prior. Uncertainty is quantified using a Laplace approximation to the posterior. Although this shrinkage does not affect which genes are identified as significantly differentially expressed, it yields more reliable effect size estimates for downstream analyses such as visualisation, gene filtering, and functional enrichment (16).

In **DESeq2**, differential expression is assessed using a Wald test on the maximum likelihood estimates of log-fold changes (LFCs), testing the null hypothesis  $H_0 : \beta_{ik} = 0$  against the alternative  $\beta_{ik} \neq 0$ . Although a zero LFC may be biologically unlikely due to complex gene regulatory networks, it provides a practical baseline for statistical testing, especially in small-scale studies like ours with only three replicates per condition (12). P-values are adjusted for multiple testing using the Benjamini–Hochberg procedure to control the false discovery rate (FDR) (17). Due to limited statistical power, we use an adjusted p-value threshold of 0.1 to determine significance.

As discussed in Section 2.2, **DESeq2** performs independent filtering by default, using the mean of normalised counts to exclude genes with low expression. The filtering threshold is automatically chosen to maximise discoveries at the target false discovery rate (FDR), set here at 0.1. This filter is independent of the test statistic under the null hypothesis, enhancing statistical power (6). Additionally, **DESeq2** incorporates automatic outlier detection based on Cook’s distance, flagging observations exceeding the 99th percentile of the  $F(q, q-n)$  distribution, where  $q$  is the number of model parameters and  $n$  the number of samples. Outlier handling depends on sample size: it is skipped for conditions with two or fewer replicates; genes with outliers are excluded when there are six or fewer replicates; and for seven or more replicates, outliers are replaced with imputed values via trimmed means before refitting the model.

The rlog transformation, introduced in Section 2.3, converts raw counts  $c_{ij}$  for gene  $i$  in sample  $j$  to  $\log_2(q_{ij}) = \beta_{i0} + \beta_{ik}$ , fitting a model similar to Equation 2.1 and applying empirical Bayes shrinkage to the log-fold changes relative to baseline expression  $\beta_{i0}$ . By default, **DESeq2** uses blind dispersion estimation for rlog, ignoring experimental design and

treating all samples as replicates of a single condition. This makes rlog-transformed data suitable for unsupervised analyses like quality control, minimizing experimental group effects. The VST transformation is also blinded by default.

Our downstream analysis focused on the four interaction terms  $\beta_{i6}$  to  $\beta_{i9}$  in Equation 2.1 to identify genes whose stress response is modulated by the presence or absence of the FLC1 gene, while also considering main effects. To assess model fit, we examined the dispersion plot, expecting gene-wise dispersions to scatter around the fitted mean-dependent trend, with dispersion decreasing as mean expression increases (16). After multiple testing, the p-value distribution was inspected; a well-calibrated test should show a spike near zero and a flat distribution elsewhere (18). We produced MA plots for both unshrunken and shrunken LFCs, highlighting significant and non-significant genes to visualise fold change magnitude and distribution across expression levels (16). Volcano plots displayed the top 10 most significant genes by adjusted p-value.

We compared the significant gene sets for the interaction terms by assessing both the number of genes per interaction and their overlaps. To identify shared expression patterns, we selected the top 500 most variable genes across samples for all interactions and performed hierarchical clustering on the correlation matrix of z-scores derived from normalised counts. For this, rlog and VST transformations were applied without blinding, using the design matrix to estimate dispersions. The optimal cluster number was determined via the Gap statistic (19). Cluster expression profiles were visualised through heatmaps and line plots to illustrate expression trends across experimental conditions.

## 2.6 Software

All analyses were performed using R version 4.4.1. Differential expression analysis was conducted with the DESeq2 package, version 1.46.0. The complete code for reproducing the analysis and generating this report is available at <https://github.com/dievillano/gene-expression>.

# 3 Results

Gene-wise total read counts ranged from 0 to 2.97 million, with gene CNAG\_06125 showing the highest total count across all samples. A total of 25 out of 6795 genes had zero total counts. Library sizes (i.e., total read counts per sample) ranged from 4.26 to 9.02 million, with sample S12 from condition FL-Y-37 having the largest library. At the condition level, WT-Y-30 showed the highest total library size (25.93 million). A barplot of library sizes across samples is shown in Figure S4.1, highlighting variability across libraries and the need for normalisation prior to comparing expression levels.

## 3.1 Pre-processing

After pre-filtering, we retained 6613 genes (97.32%), removing 182 genes and moderately reducing the multiple testing burden for DE analysis. We applied CPM normalisation followed by  $\log_2$ -CPM, rlog, and VST transformations on the filtered count matrix as described in Section 2.3. Figure S4.2 presents boxplots of expression values by sample and condition for each transformation. CPM alone did not stabilise variance, showing skewed distributions with many outliers. In contrast,  $\log_2$ -CPM, rlog, and VST reduced skewness and improved centring, though some outliers remain. Among these, rlog and VST yielded more uniform distributions across samples compared to the simple log transform, which has known limitations (see Section 2.3). The impact on variance stabilisation is further illustrated in Figure S4.3, which plots gene-wise standard deviations against ranked mean expression for each transformation. CPM displays a pronounced variability peak at high expression levels, whereas transformed data show flatter trends, indicating effective variance stabilisation across the expression range.

## 3.2 Quality assessment and exploratory analysis

PCA was performed on the transformed data of the genes at the 10% of highest variance, yielding an optimal number of three components for all methods except CPM, which retained only one. These components explained 92.86%, 93.19%, and 92.71% of the total variance for  $\log_2$ -CPM, rlog, and VST, respectively, while CPM explained only 75.19%. The scree plot for the rlog-transformed data, shown in Figure S4.4, illustrates the retained components and their associated variance. The score plots for all retained component pairs in Figure S4.5 show that replicates from the same condition cluster tightly, indicating high consistency and replicate quality. Since the rlog and VST transformations yield similar explained variance (slightly higher for rlog) we will present results based on the rlog-transformed data from this point forward.

In Figure 3.1, subplot A1, samples separate clearly by strain along PC1 and by media condition along PC2. Notably, samples from conditions Y and YC, as well as YE and YCE, cluster closely together, suggesting that EGTA primarily drives the observed separation rather than CFW. This distinction between samples with and without EGTA is

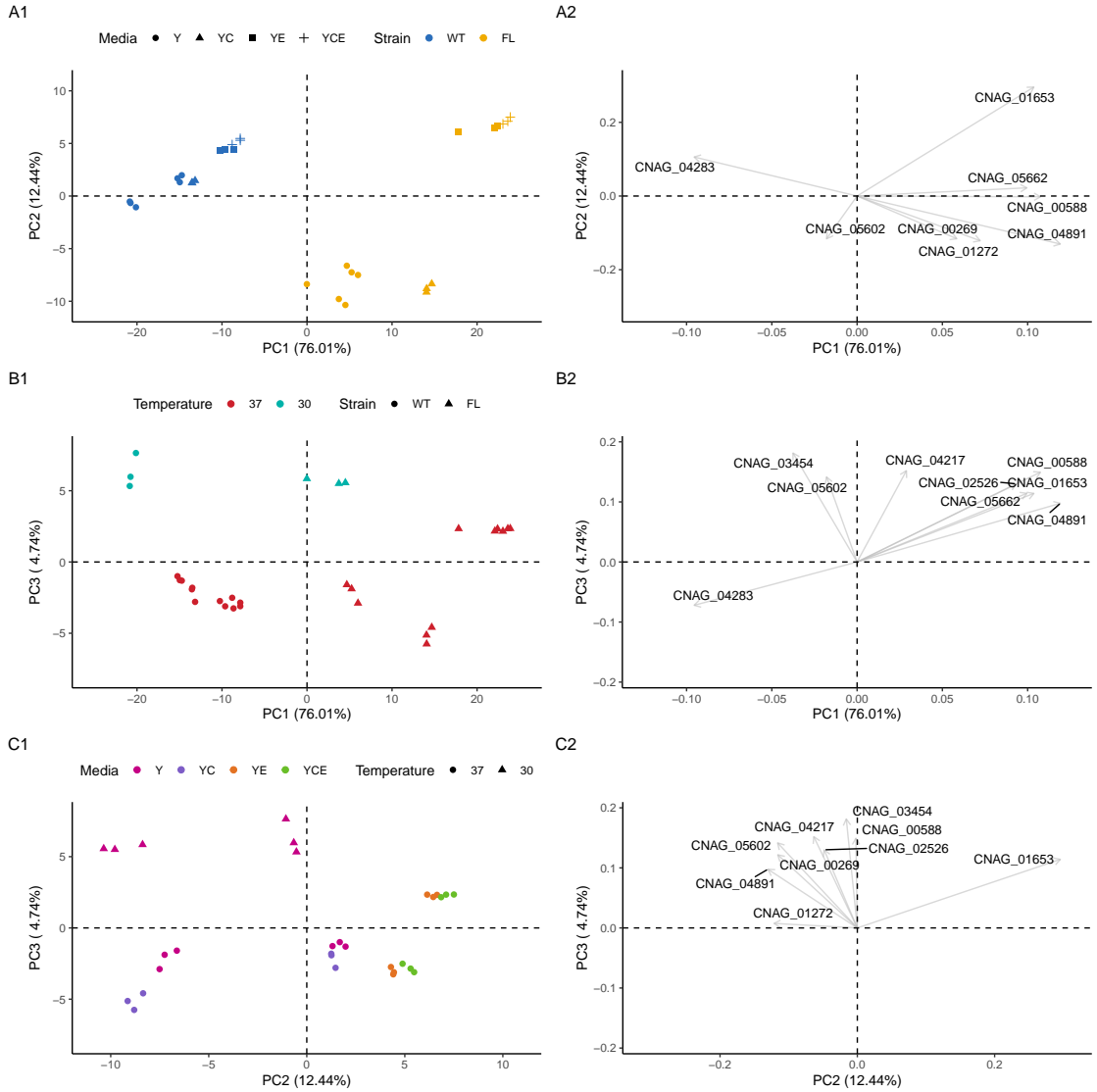


**Figure 3.1:** Sample projections onto pairs of principal components: (A) PC1 vs PC2, (B) PC1 vs PC3, and (C) PC2 vs PC3. Subplots labeled 1 display sample scores coloured and shaped by relevant experimental conditions, while subplots labeled 2 show loadings of the top 10 genes with the highest absolute loadings on each component pair.

more pronounced in the FLC1 $\Delta$  strain compared to the WT strain. Additionally, a clear separation between samples grown in Y and YC media is observed only for the FLC1 $\Delta$  strain, indicating a potential interaction between strain and growth media.

Subplot A2 shows that genes CNAG\_04283 and CNAG\_05602 mainly drive separation toward the WT strain, with CNAG\_04283 having the strongest effect as expected since it corresponds to the FLC1 gene itself. Genes CNAG\_05662 and CNAG\_00588 align closely with FLC1 $\Delta$  samples, while CNAG\_00269, CNAG\_01272, and CNAG\_04891 appear to contribute to the separation of FLC1 $\Delta$  samples grown in Y and YC media. Notably, CNAG\_01653 is strongly associated with FLC1 $\Delta$  samples grown with EGTA, suggesting a gene-specific response to this condition.

In subplot B1, samples separate by temperature along PC3, with further strain-specific separation within each temperature group, suggesting a potential interaction between these factors. Subplot B2 reveals that CNAG\_04217 drives the separation of FLC1 $\Delta$  samples at 30°C, while CNAG\_02526, CNAG\_05662, CNAG\_01653, CNAG\_00588, and CNAG\_04891 contribute to the separation of FLC1 $\Delta$  samples at 37°C. Conversely, CNAG\_03454 and CNAG\_05602 drive separation toward WT samples at 30°C, with CNAG\_04283 (FLC1 gene) driving separation toward WT samples at 37°C.

Finally, subplot C1 shows temperature-driven separation along PC3 and media-driven separation along PC2. In subplot C2, most genes with strong loadings on these components associate with samples grown at 30°C in YPD, while CNAG\_01653 notably contributes to the separation of samples grown at 37°C in YE and YCE media conditions.

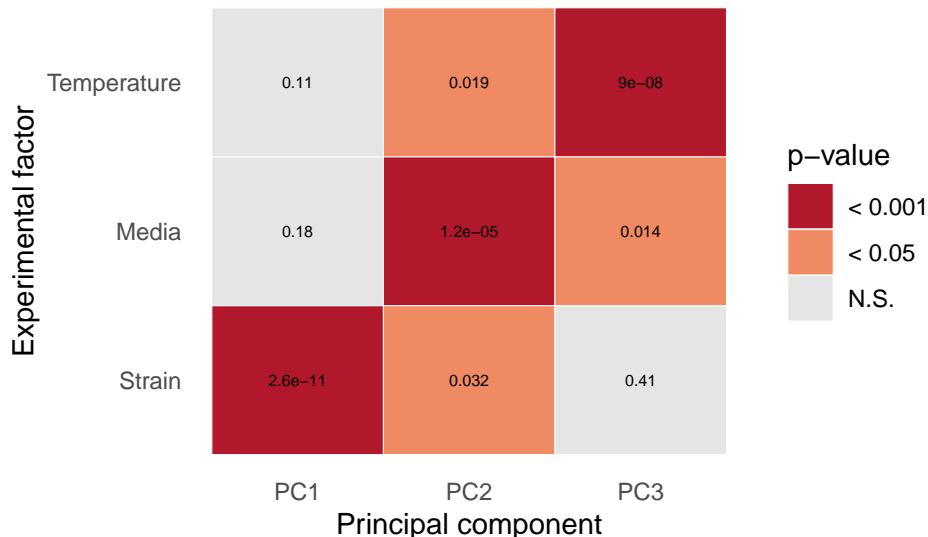


**Figure 3.2:** Heatmap of ANOVA p-values testing the association between principal components and experimental factors.

The results of the pairwise ANOVA tests between the retained principal components and experimental factors (Figure 3.2) show that PC1 primarily captures variation associated with the strain condition. PC2 is influenced by all three experimental factors, with the strongest association observed for the media condition. PC3 reflects separation driven by both media and temperature, with the most significant effect corresponding to temperature. The top 10 genes contributing most strongly to each principal component are shown in Figure 3.3. Notably, CNAG\_01653 exhibits the largest loading magnitude overall, particularly in PC2, and also shows substantial contributions to PC1 and PC3. CNAG\_04283,

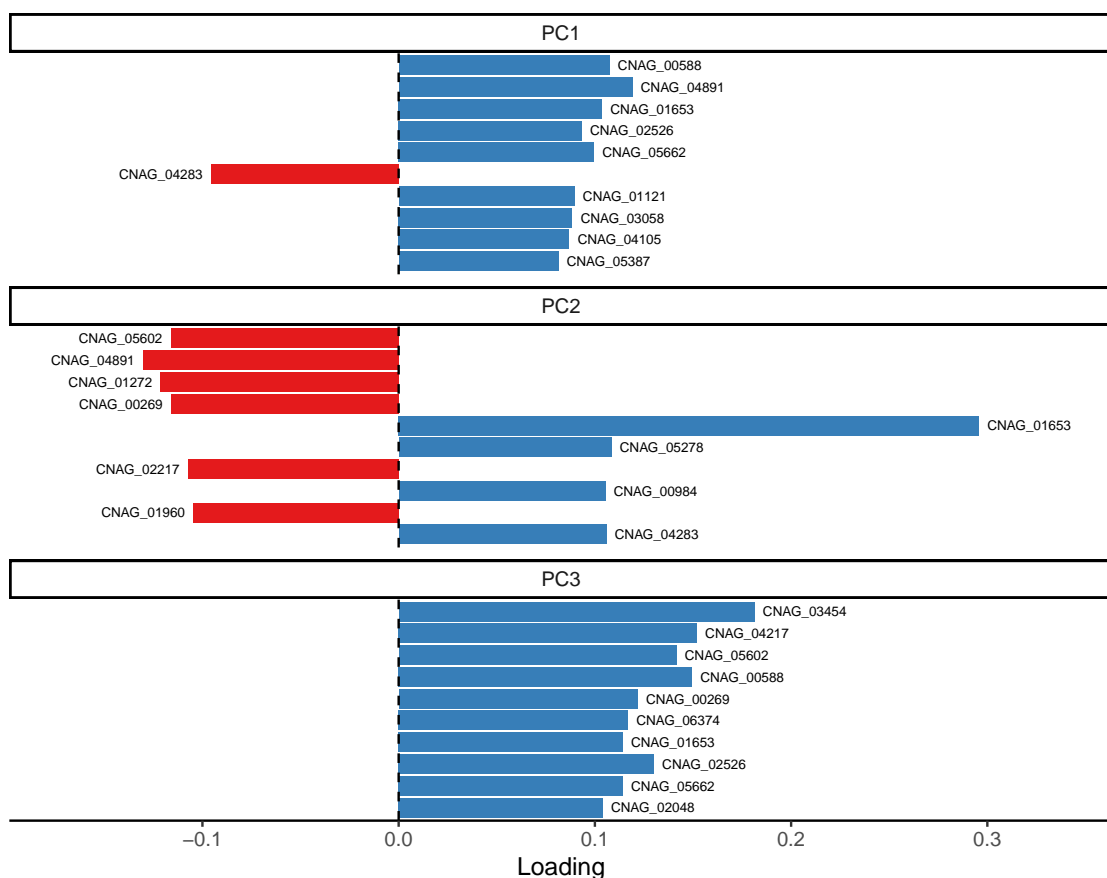


**Figure 3.3:** Barplots displaying the top 10 genes with the highest absolute loadings for each principal component.

**Table 3.1:** Number and percentage of upregulated and downregulated genes identified at an FDR threshold of 0.1 for each contrast tested, along with the total number of DE genes.

Contrast	Upregulated	Downregulated	Total
Strain (FL) + Media (YC)	476 (37.96%)	778 (62.04%)	1254 (100%)
Strain (FL) + Media (YCE)	955 (42.96%)	1268 (57.04%)	2223 (100%)
Strain (FL) + Media (YE)	848 (48.02%)	918 (51.98%)	1766 (100%)
Strain (FL) + Temperature (30)	421 (36.39%)	736 (63.61%)	1157 (100%)

which encodes the FLC1 gene, contributes strongly to both PC1 and PC2. Another prominent gene, CNAG\_04891, is among the top contributors to both PC1 and PC2 as well. For PC3, CNAG\_03454 shows the highest association, followed by CNAG\_04217 and CNAG\_00588, the latter also contributing notably to PC1.

### 3.3 Differential expression analysis

Moving on to model fitting for DE analysis, we observed that the shrunk dispersion estimates aligned well with the mean-dependent trend, indicating a good overall fit (Figure S4.6). This pattern was more consistent in the filtered dataset, whereas in the unfiltered dataset, the trend appeared to be overly influenced by genes with low mean expression levels.

The contrasts used to test the significance of the model coefficients (excluding the intercept), which correspond to the log-fold changes (LFCs), were labelled to reflect both the main effects and interaction terms included in the DE analysis. Main effects included “Strain (FL)” for the FLC1 $\Delta$  strain versus WT, “Media (YC)”, “Media (YE)”, and “Media (YCE)” for the addition of CFW, EGTA, and both to YPD, respectively, and “Temperature (30)” for growth at 30°C versus 37°C. Interaction terms were labelled as “Strain (FL) + Media (YC)”, “Strain (FL) + Media (YE)”, and “Strain (FL) + Media (YCE)” to capture the combined effect of strain and media condition, and “Strain (FL) + Temperature (30)” for the interaction between strain and temperature. As previously mentioned, our analysis focused on the interaction terms. Unless otherwise noted, results are based on the filtered dataset.

The (unadjusted) p-value histograms for each contrast display the expected uniform distribution under the null hypothesis, indicating a well-calibrated multiple testing procedure (Figure S4.7). Similar results were observed for the unfiltered dataset (not shown). No outliers were detected in any contrast. However, 129 genes (1.95%) were automatically removed due to low mean normalized counts during the testing of the Strain (FL) + Media (YC) term, as part of DESeq2’s independent filtering procedure. MA plots for all contrasts showed a uniform distribution of significantly upregulated and downregulated genes across the range of mean expression levels, suggesting that the procedure is not biased towards highly expressed genes (Figure S4.8).

The Strain (FL) + Media (YCE) contrast yielded the highest number of differentially expressed (DE) genes (2223), while Strain (FL) + Temperature (30) had the fewest (767) (Table 3.1). All contrasts showed more downregulated than upregulated genes. The highest percentage of downregulated genes was observed in Strain (FL) + Temperature (30) (63.61%), although the contrast with the greatest absolute number of downregulated genes was Strain (FL) + Media (YCE) (1268). The highest proportion of upregulated genes was found in Strain (FL) + Media (YE) (48.02%), while the highest count of upregulated genes overall was again seen in Strain (FL) + Media (YCE) (955) (Table 3.1). The Strain

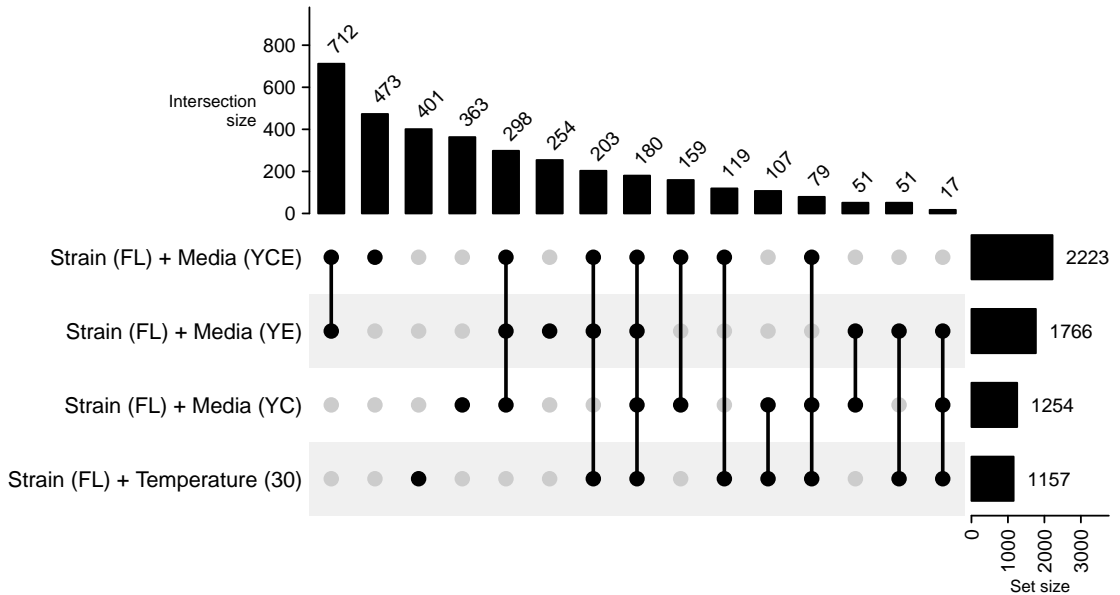


**Figure 3.4:** UpSet plot illustrating the intersections between differentially expressed (DE) gene sets across the various contrasts.

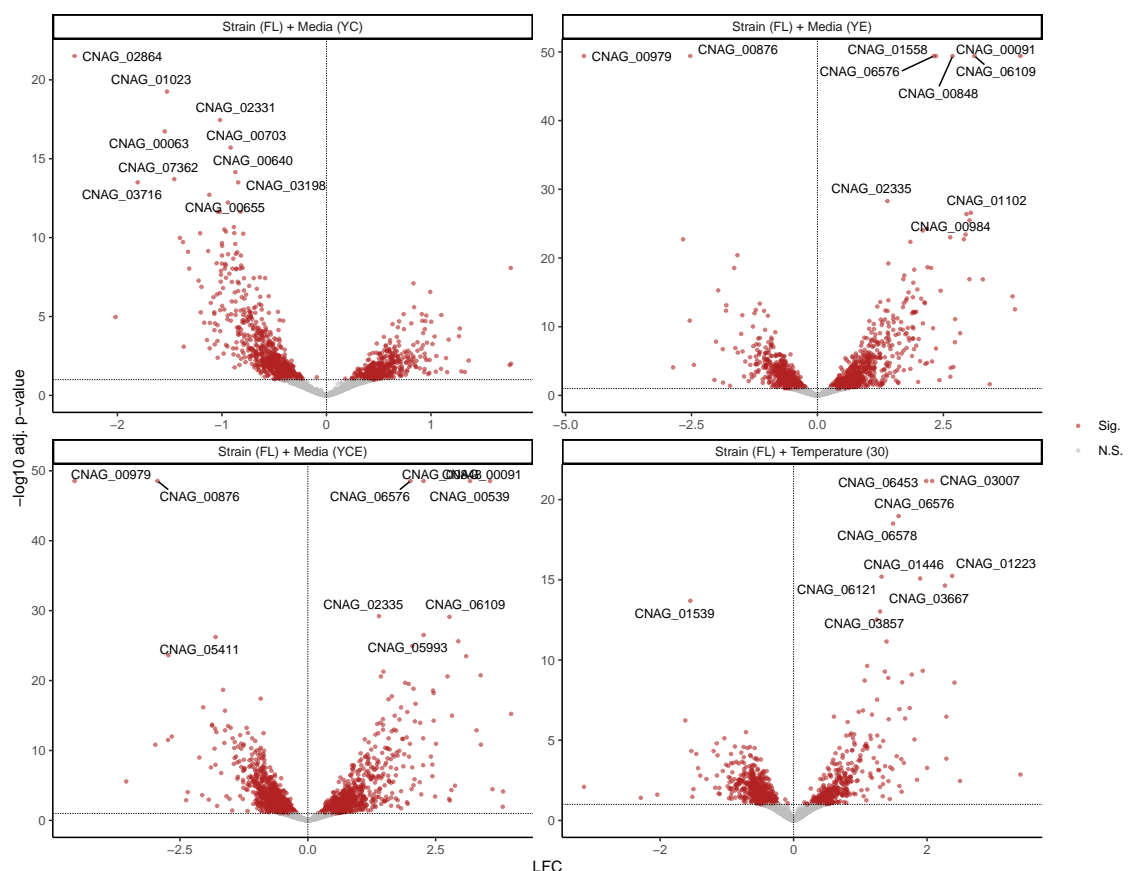
(FL) + Media (YCE) and Strain (FL) + Media (YE) contrasts shared the highest number of differentially expressed (DE) genes in common (712). In total, 3467 uniquely genes were identified as differentially expressed (52.43%), with 180 (2.72%) of them consistently differentially expressed across all contrasts (Figure 3.4). Strain (FL) + Media (YCE) also had the greatest number of uniquely identified DE genes (473), i.e. those not shared with any other contrast. This was followed by Strain (FL) + Temperature (30) (401), Strain (FL) + Media (YC) (363), and Strain (FL) + Media (YE) (254).

Figure 3.5 highlights the top 10 most significant genes for each contrast. Notably, all of the top genes for the Strain (FL) + Media (YC) interaction were downregulated, while all but one of the top genes for the Strain (FL) + Temperature (30) interaction were upregulated. Gene CNAG\_06556 appeared most frequently among the top genes, being significantly differentially expressed in all contrasts except Strain (FL) + Media (YC). In addition, genes CNAG\_00091, CNAG\_00848, CNAG\_00876, CNAG\_00979, and CNAG\_02335 were consistently ranked among the top genes in both the Strain (FL) + Media (YE) and Strain (FL) + Media (YCE) contrasts.

### 3.4 Gene expression profiles

The optimal number of clusters for the top 500 differentially expressed (DE) genes with the highest variance, determined by the Gap statistic, was four when using z-scores of the rlog-transformed data (Figure S4.9). The same optimal cluster number was obtained with VST-transformed data, whereas the  $\log_2$ -CPM transformation resulted in an uninformative single cluster, indicating it may be less effective at capturing meaningful expression patterns in this context.

Figure 3.6 displays a heatmap of the z-scored expression values across the four clusters (labelled 1–4). Because the data are z-scored, positive values indicate expression above the gene's mean across all conditions, while negative values indicate below-average expression. Cluster 1 is distinct, with genes showing above-average expression in the WT strain and



**Figure 3.5:** Volcano plots for each contrast highlighting the top 10 most significant genes based on adjusted p-values and log<sub>2</sub> fold changes.

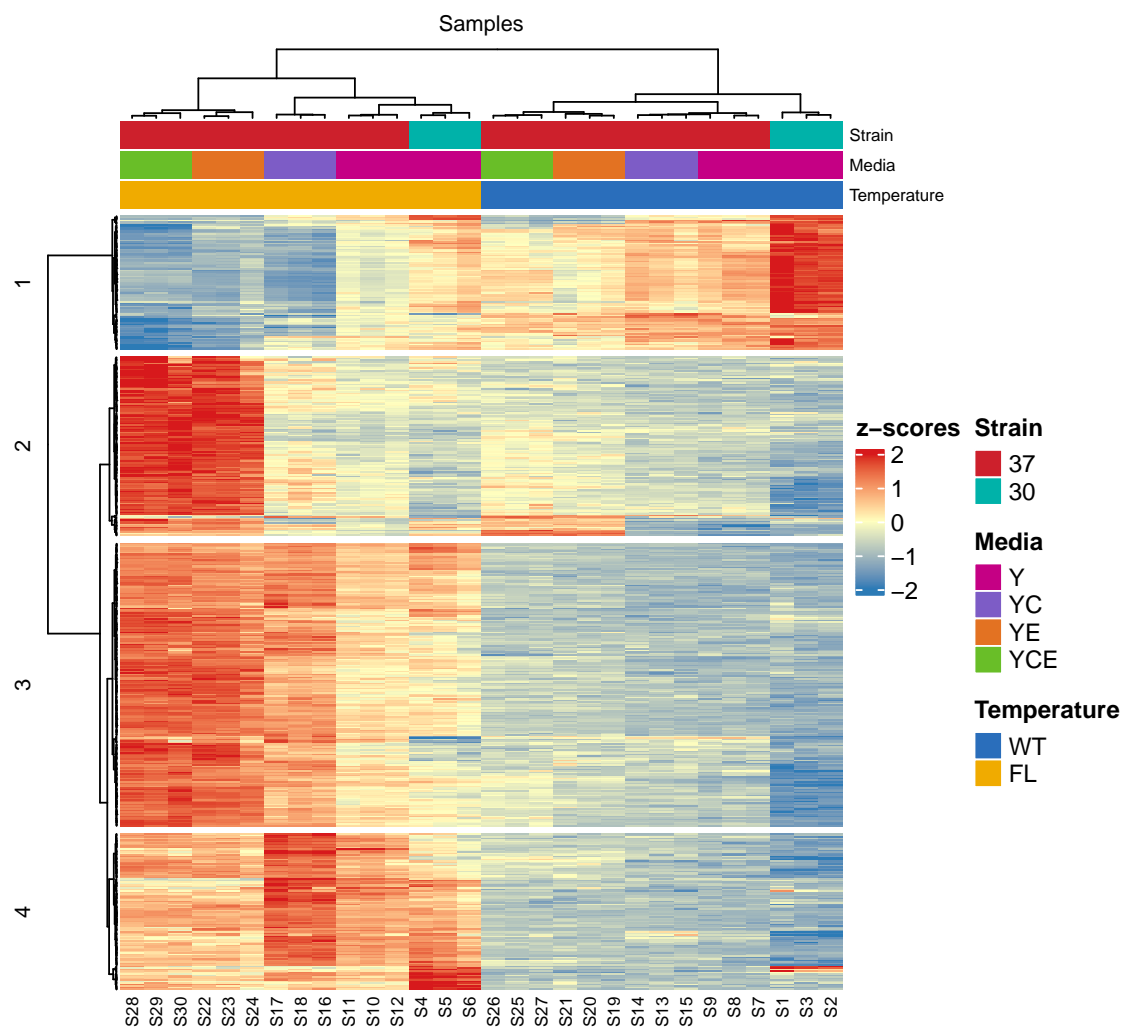


**Figure 3.6:** Heatmap of z-scored expression levels for the top 500 most variable genes, annotated by cluster membership and experimental conditions.

below-average expression in the  $FLC1\Delta$  strain, particularly under the WT-Y-30 basal condition. In contrast, clusters 2–4 exhibit the opposite pattern, with genes generally showing lower expression in WT and higher expression in  $FLC1\Delta$  samples, suggesting a strain-specific shift in relative expression. Within these, cluster 2 genes tend to be upregulated in FL-YE-37 and FL-YCE-37 conditions but near or below average in other  $FLC1\Delta$  combinations. Cluster 3 follows a similar pattern but with elevated expression across a broader range of  $FLC1\Delta$  conditions. Cluster 4 displays an inverse trend to cluster 2, with higher expression at FL-Y-30, FL-Y-37, and FL-YC-37 conditions.

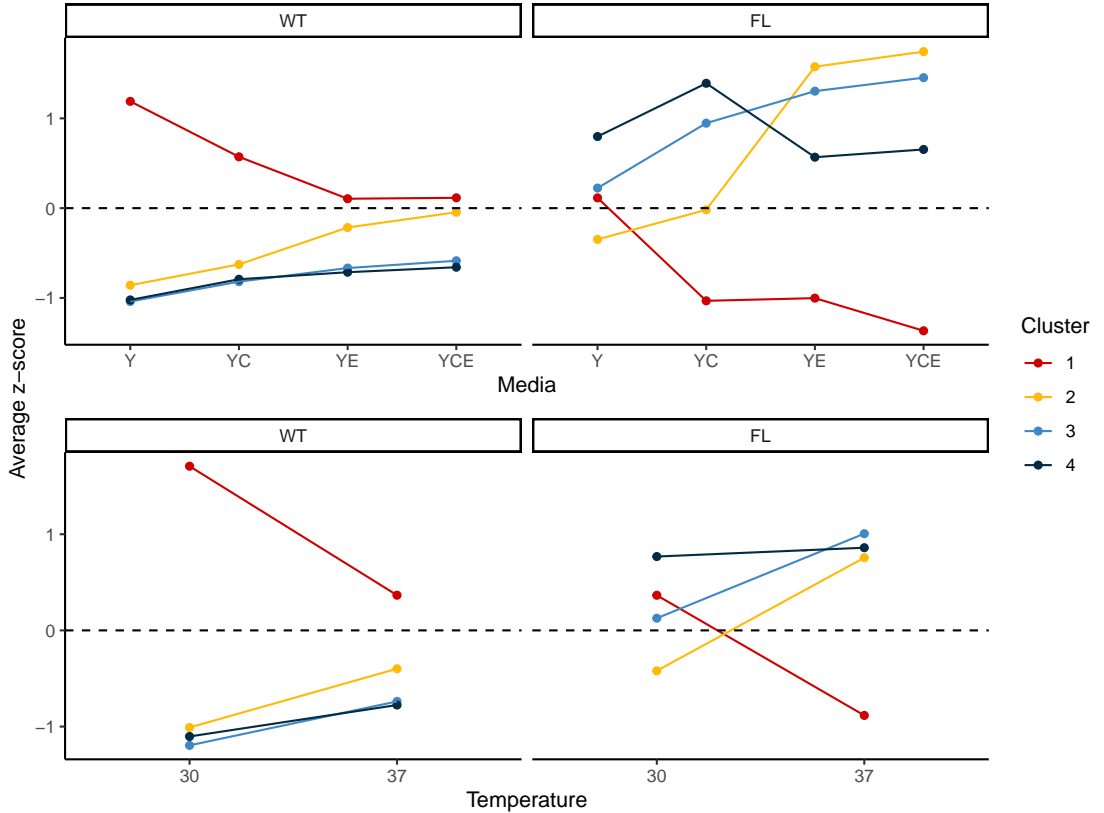


**Figure 3.7:** Line plot of average z-scored expression for each gene cluster across growth media and temperature conditions, faceted by strain (WT and  $FLC1\Delta$ ).

Figure 3.7 illustrates the average z-scored expression patterns of the four gene clusters across media and temperature conditions, shown separately for the WT and  $FLC1\Delta$  (FL) strains. In the WT strain (top-left panel), cluster 1 genes consistently exhibit above-average expression across all media, with the highest levels observed in the Y media condition. Expression gradually decreases through YC and YE to YCE, with a more pronounced drop from Y to YC than from YE to YCE. Conversely, clusters 2, 3, and 4 show consistently below-average expression in WT, though expression slightly increases with the addition of CFW and EGTA.

For the FL strain (top-right panel), expression patterns invert. Cluster 1 genes are below average in all media and show a marked decrease when CFW and EGTA are present (from Y to YC, and from YE to YCE). Clusters 2 and 3 exhibit progressively increasing expression across media, particularly in YE and YCE. Cluster 2 displays a strong increase with EGTA addition, whereas cluster 3 follows a similar trend but with a less pronounced rise. Cluster 4 shows increased expression upon CFW addition (from Y to YC and from YE to YCE), especially in the Y medium, but has the lowest expression in EGTA-containing

growth media.

Regarding temperature, in the WT strain (bottom-left panel), cluster 1 genes remain above average at both 30°C and 37°C, but with reduced expression at 37°C. Clusters 2–4 remain below average, though expression levels increase with temperature. In the FL strain (bottom-right panel), the patterns again invert: cluster 1 genes show near or below-average expression, decreasing further at 37°C. Clusters 2 and 3 show near or above-average expression that increases with temperature, while cluster 4 maintains above-average expression with little change across temperatures.

### 3.5 Gene prioritization

To prioritise the most informative genes, we ranked the 500 genes used for clustering based on two criteria: smallest adjusted p-value and largest absolute log<sub>2</sub> fold change (LFC), then computed an average rank across both metrics. The top 100 genes according to this combined ranking are shown in Figure 3.8, which presents a heatmap of their LFCs across all contrasts alongside their cluster membership. This plot provides a comprehensive summary, integrating statistical significance, expression changes, and clustering results to identify candidate genes of interest. For example, CNAG\_04469, which appears near the top of the heatmap, is significantly differentially expressed in the interaction between strain and media at the YE and YCE levels, but not at other contrasts. In both cases, this gene is upregulated in the FL strain relative to the WT-Y-37 reference. As a member of cluster 2, its expression profile aligns with that described for cluster 2 genes in Figure 3.7. Additionally, many of the top-ranked genes exhibit significant LFCs specifically in the YE and YCE conditions, with significance in one condition often accompanied by significance in the other.

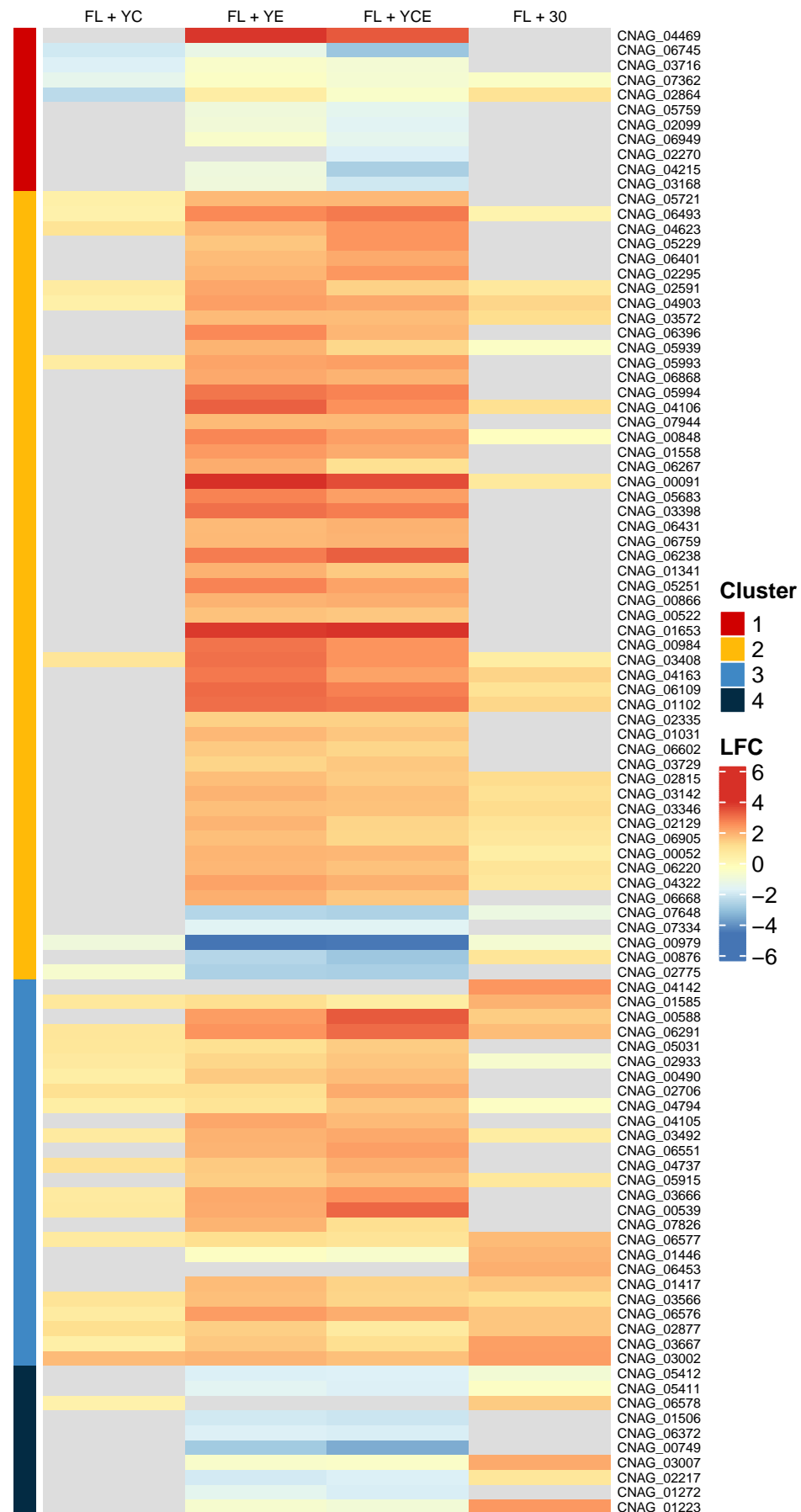


**Figure 3.8:** Heatmap of log2 fold changes for the top 100 ranked genes across all contrasts, with cluster membership indicated.

## 4 Conclusions

This report presents the analysis of RNA-Seq data from an experiment investigating the response of *Cryptococcus neoformans* to cell wall stress across various environmental and genetic conditions, focusing on the FLC1 gene, a promising antifungal drug target. The study aimed to provide statistically robust insights into transcriptomic responses to combinations of growth media (CFW, EGTA, or both), temperature (30°C and 37°C), and the presence or absence of FLC1. The objectives were to assess replicate consistency, explore broad expression patterns among samples, identify differentially expressed genes across conditions, and reveal structured expression profiles within those genes.

Replicates clustered closely in PCA, indicating good biological consistency. Samples grown in YPD and YPD + CFW, as well as YPD + EGTA and YPD + CFW + EGTA, clustered together, but similarity varied by strain. In the FLC1 $\Delta$  strain, adding CFW caused greater expression changes than in WT, with distinct profiles especially in YPD + CFW. Genes driving these patterns included CNAG\_04283 (FLC1), CNAG\_01653, CNAG\_04891, and CNAG\_00588. At 37°C, the FLC1 $\Delta$  strain showed more expression variation across media, while at 30°C, greater overall divergence was observed. However, PCA loadings alone do not confirm differential expression for individual genes.

About 52.4% of genes (3,467) were differentially expressed in strain-media and strain-temperature contrasts relative to WT at 37°C in YPD. The greatest number of DE genes occurred in the FLC1 $\Delta$  strain at 37°C with YPD + CFW + EGTA, mostly downregulated, with the highest downregulation (62%) seen in FLC1 $\Delta$  at 37°C in YPD + CFW. Gene CNAG\_06576 was consistently significant, generally upregulated except for downregulation in that latter condition. Clustering the top 500 most variable DE genes identified four groups: cluster 1 genes were expressed above average in WT and below average in FLC1 $\Delta$ , while clusters 2–4 showed the opposite pattern, indicating a strain-specific expression shift. Cluster 1 genes had higher expression under basal conditions (YPD, 30°C) and lower under stress (CFW, EGTA, 37°C), with clusters 2–4 displaying inverse trends more marked in FLC1 $\Delta$ . Notably, cluster 4 genes decreased expression with EGTA and were largely unaffected by temperature. In addition, a ranked list of the top 100 DE genes with cluster annotations is provided for future study.

One limitation of this analysis is the reliance on a single algorithm for detecting differentially expressed genes, specifically the method implemented in the `DESeq2` package. The robustness of the findings presented in this report could be further evaluated by applying alternative differential expression analysis methods.

## References

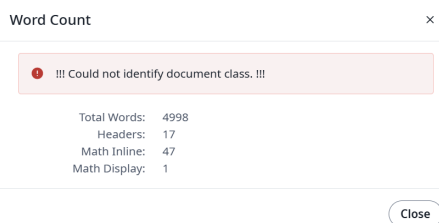
1. May RC, Stone NR, Wiesner DL, Bicanic T, Nielsen K. Cryptococcus: From environmental saprophyte to global pathogen. *Nature Reviews Microbiology*. 2016;14(2):106–17.
2. Stempinski PR, Goughenour KD, Plooy LM du, Alspaugh JA, Olszewski MA, Kozubowski L. The cryptococcus neoformans Flc1 homologue controls calcium homeostasis and confers fungal pathogenicity in the infected hosts. *Mbio*. 2022;13(5):e02253–22.
3. Wang Z, Gerstein M, Snyder M. RNA-seq: A revolutionary tool for transcriptomics. *Nature reviews genetics*. 2009;10(1):57–63.
4. Chen Y, Lun TLL, Smyth GK. [From reads to genes to pathways: Differential expression analysis of RNA-seq experiments using rsubread and the edgeR quasi-likelihood pipeline](#). F1000Research. 2016;5(1438).
5. Sha Y, Phan JH, Wang MD. Effect of low-expression gene filtering on detection of differentially expressed genes in RNA-seq data. In: 2015 37th annual international conference of the IEEE engineering in medicine and biology society (EMBC). IEEE; 2015. p. 6461–4.
6. Bourgon R, Gentleman R, Huber W. Independent filtering increases detection power for high-throughput experiments. *Proceedings of the National Academy of Sciences*. 2010;107(21):9546–51.
7. Chen Y, Chen L, Lun ATL, Baldoni P, Smyth GK. [edgeR v4: Powerful differential analysis of sequencing data with expanded functionality and improved support for small counts and larger datasets](#). Nucleic Acids Research. 2025;53(2):gkaf018.
8. Gierliński M, Cole C, Schofield P, Schurch NJ, Sherstnev A, Singh V, et al. Statistical models for RNA-seq data derived from a two-condition 48-replicate experiment. *Bioinformatics*. 2015;31(22):3625–30.
9. Dillies MA, Rau A, Aubert J, Hennequet-Antier C, Jeanmougin M, Servant N, et al. A comprehensive evaluation of normalization methods for illumina high-throughput RNA sequencing data analysis. *Briefings in Bioinformatics* [Internet]. 2012 Sep;14(6):671–83. Available from: <https://doi.org/10.1093/bib/bbs046>
10. Robinson MD, Oshlack A. A scaling normalization method for differential expression analysis of RNA-seq data. *Genome biology*. 2010;11:1–9.
11. Anders S, Huber W. Differential expression analysis for sequence count data. *Nature Precedings*. 2010;1–1.

12. Love MI, Huber W, Anders S. Moderated estimation of fold change and dispersion for RNA-seq data with DESeq2. *Genome biology*. 2014;15:1–21.
13. Hafemeister C, Satija R. Normalization and variance stabilization of single-cell RNA-seq data using regularized negative binomial regression. *Genome biology*. 2019;20(1):296.
14. Dinno A. Exploring the sensitivity of horn's parallel analysis to the distributional form of random data. *Multivariate behavioral research*. 2009;44(3):362–88.
15. Zhu A, Ibrahim JG, Love MI. Heavy-tailed prior distributions for sequence count data: Removing the noise and preserving large differences. *Bioinformatics*. 2019;35(12):2084–92.
16. Mistry M, Piper M, Liu J, Khetani R. Hbctraining/DGE\_workshop\_salmon\_online: Differential gene expression workshop lessons from HCBC (first release) [Internet]. Zenodo; 2021. Available from: <https://doi.org/10.5281/zenodo.4783481>
17. Benjamini Y, Hochberg Y. Controlling the false discovery rate: A practical and powerful approach to multiple testing. *Journal of the Royal statistical society: series B (Methodological)*. 1995;57(1):289–300.
18. The Pennsylvania State University. STAT 555: Statistical analysis of genomics data. <https://online.stat.psu.edu/statprogram/stat555>; 2025.
19. Tibshirani R, Walther G, Hastie T. Estimating the number of clusters in a data set via the gap statistic. *Journal of the royal statistical society: series b (statistical methodology)*. 2001;63(2):411–23.

# Appendix

## Word count

The total word count on the main text is 4998:



## Supplementary figures

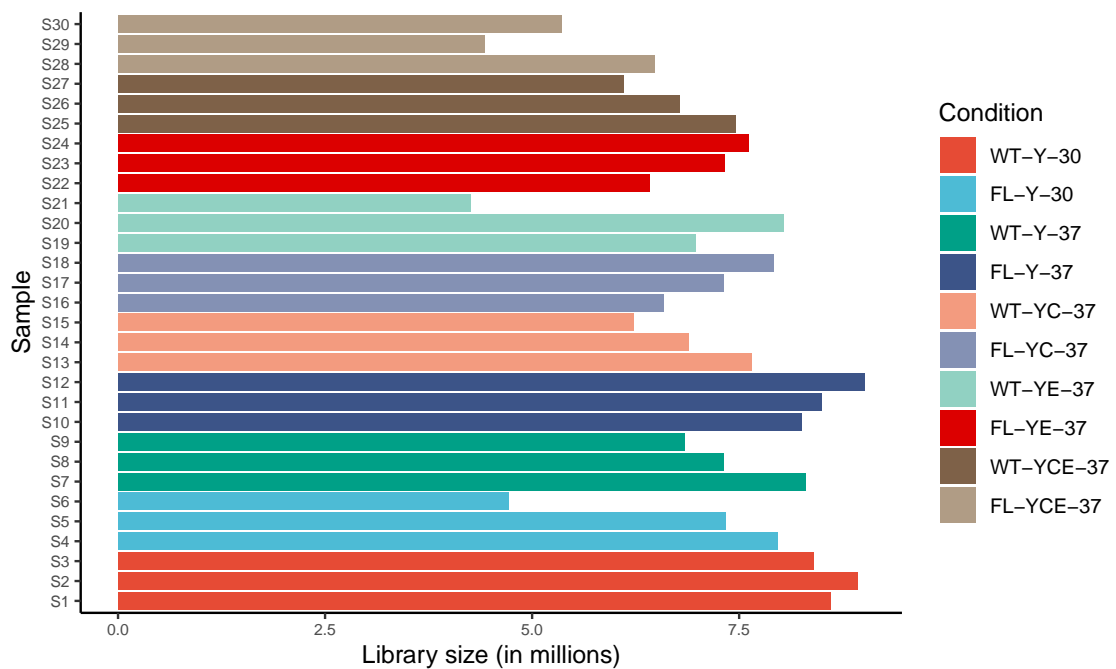


**Figure S4.1:** Barplot showing the total number of sequenced reads (in millions) per sample, with bars coloured by experimental condition.

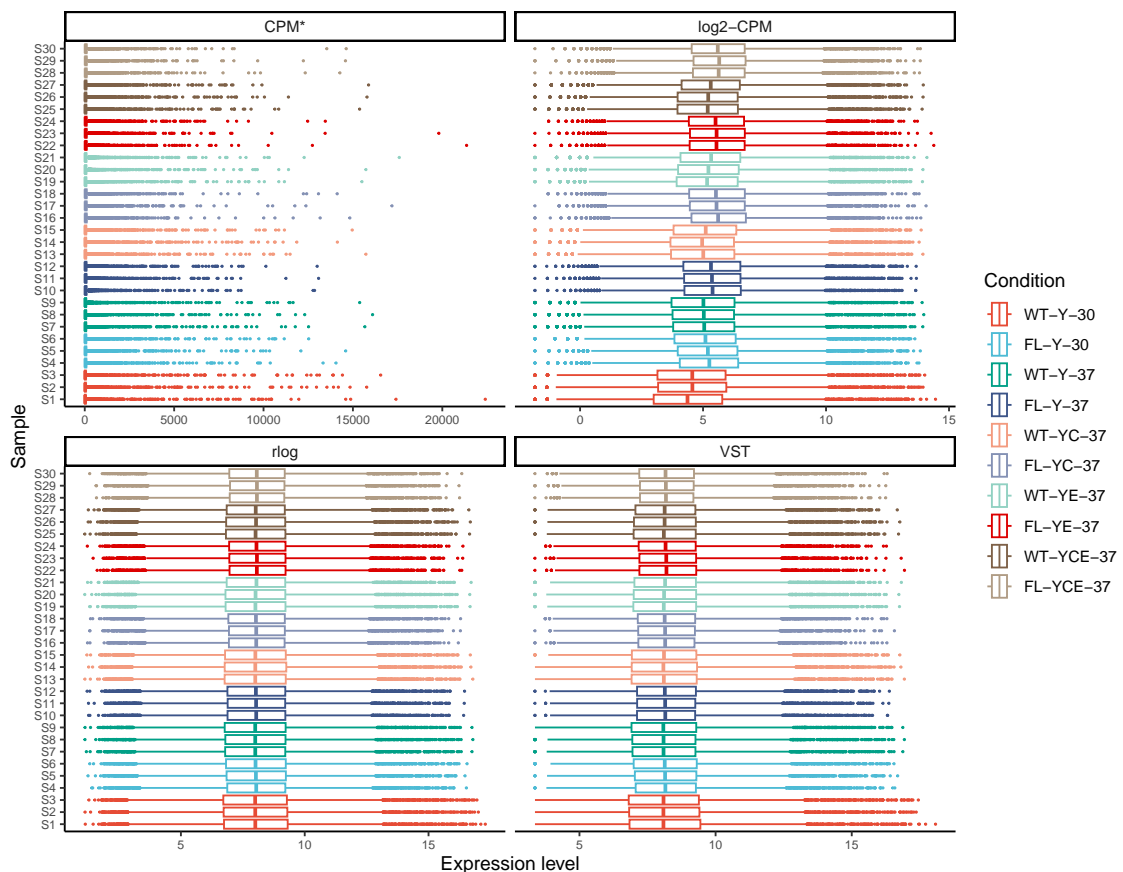


**Figure S4.2:** Boxplots of gene expression values by sample, coloured by experimental condition and faceted by transformation method. Note that CPM\* denotes normalisation only, without variance stabilisation.

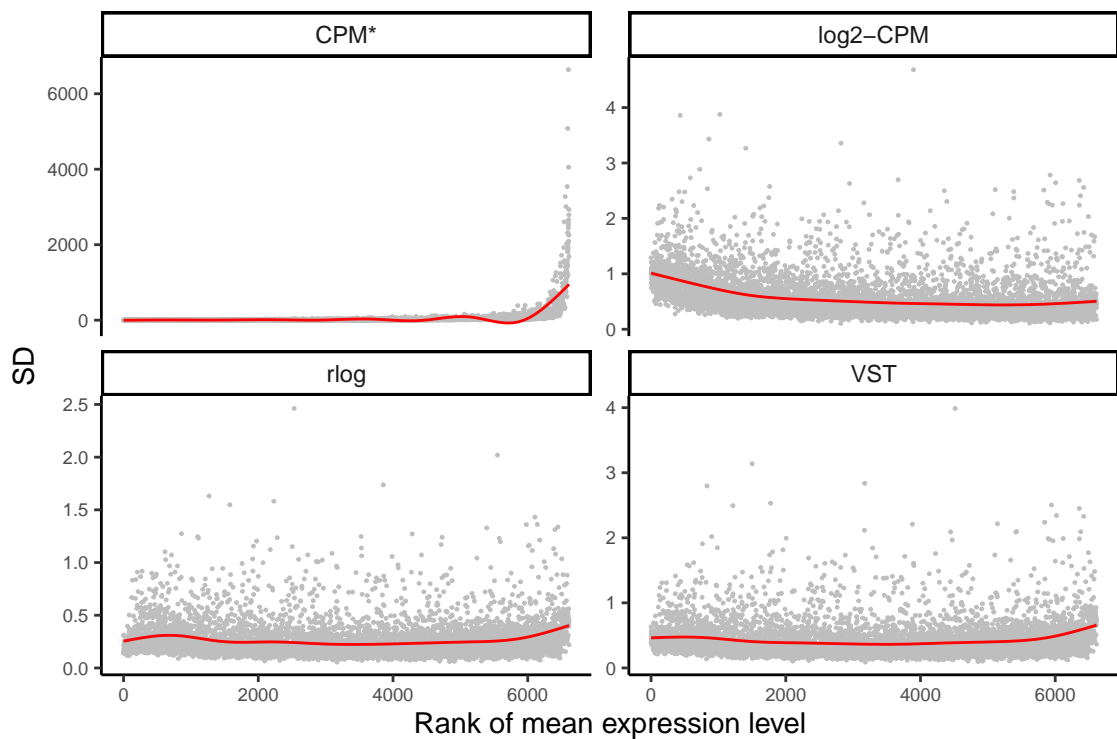


**Figure S4.3:** Mean versus standard deviation plot of gene expression values, faceted by transformation method. The red line indicates the mean-dependent trend in standard deviation. CPM\* lacks variance stabilisation, as reflected in its stronger mean–SD dependence.

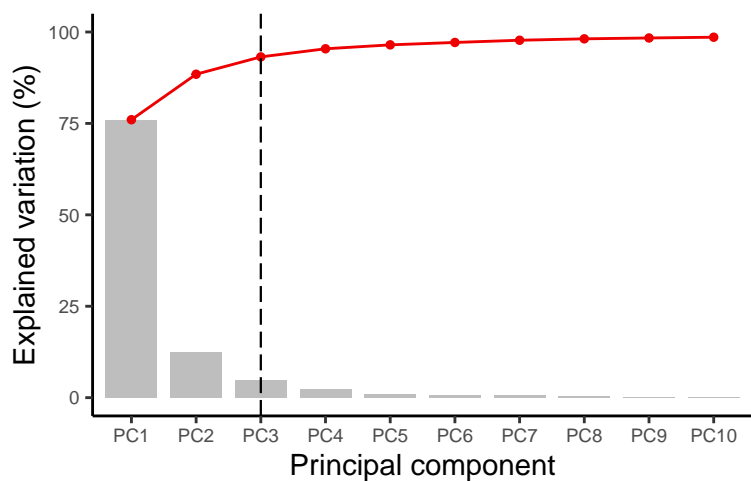


**Figure S4.4:** Scree plot of the rlog-transformed data showing the number of retained principal components based on parallel analysis.

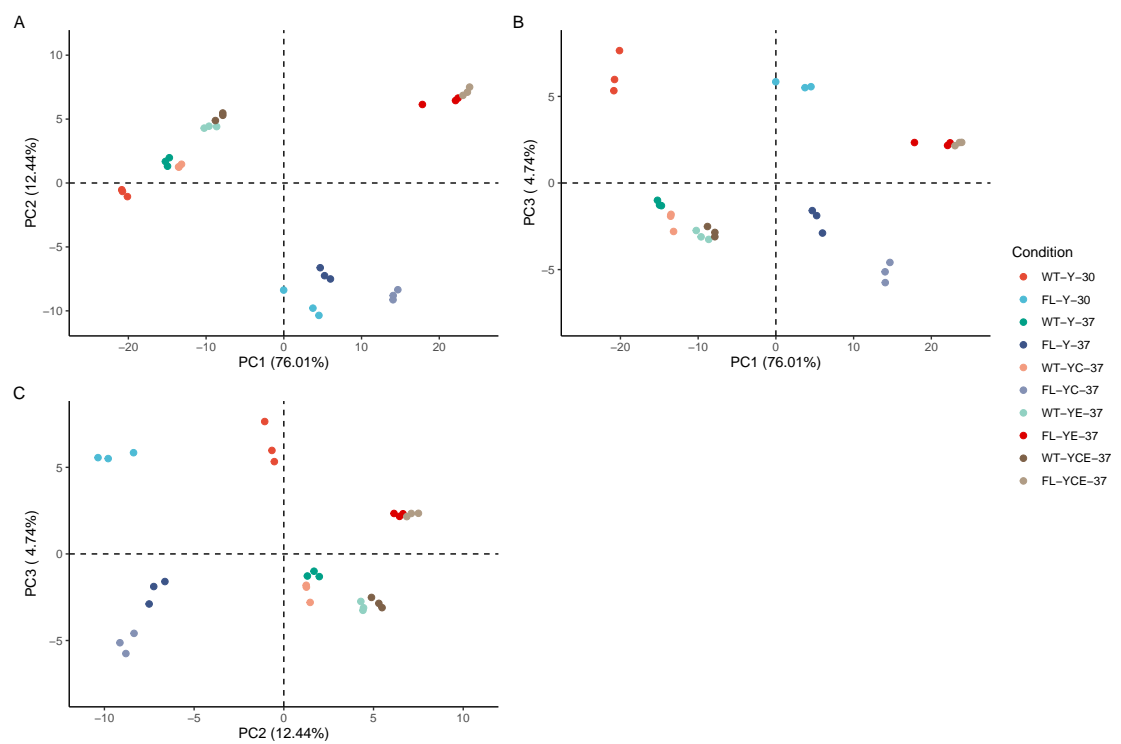


**Figure S4.5:** Samples projected onto pairwise combinations of retained principal components from rlog-transformed data, coloured by experimental condition.

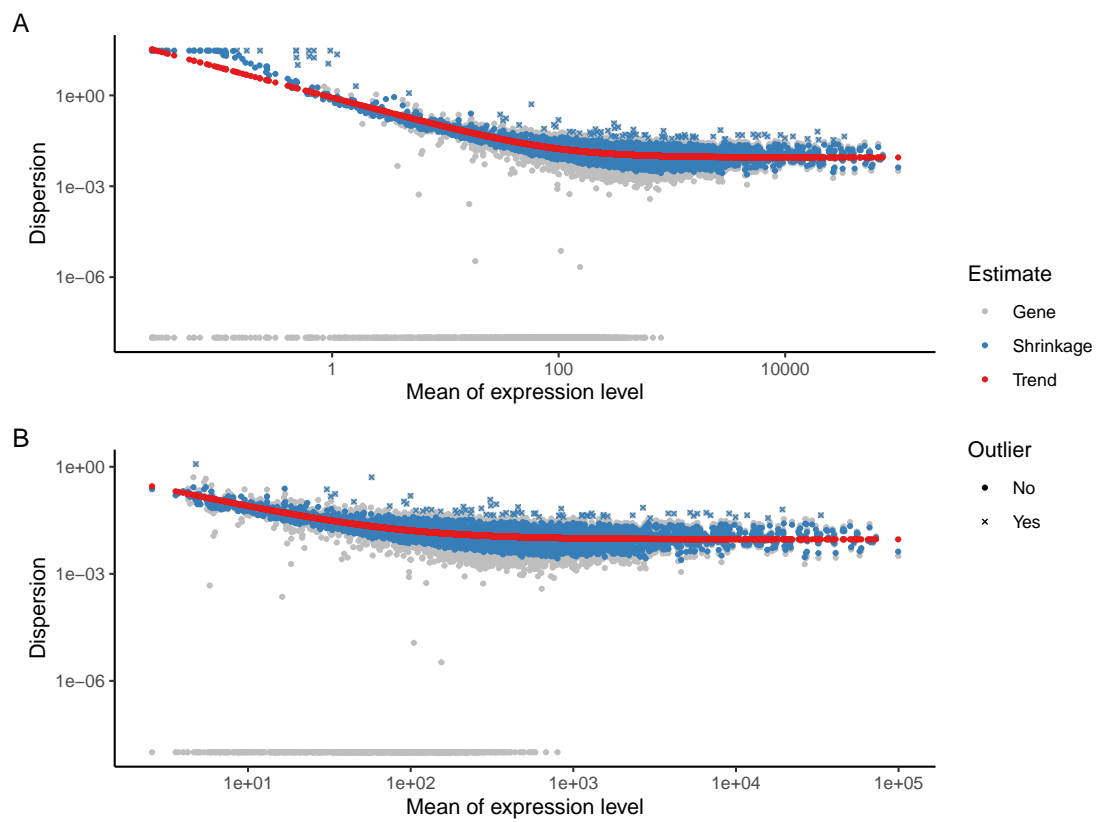


**Figure S4.6:** Dispersion estimates plotted against mean expression levels. Gray points represent gene-wise dispersion estimates, blue points show shrinkage-based estimates, and the red line indicates the mean-dependent trend. Panel (A) corresponds to unfiltered data, while panel (B) shows filtered data.

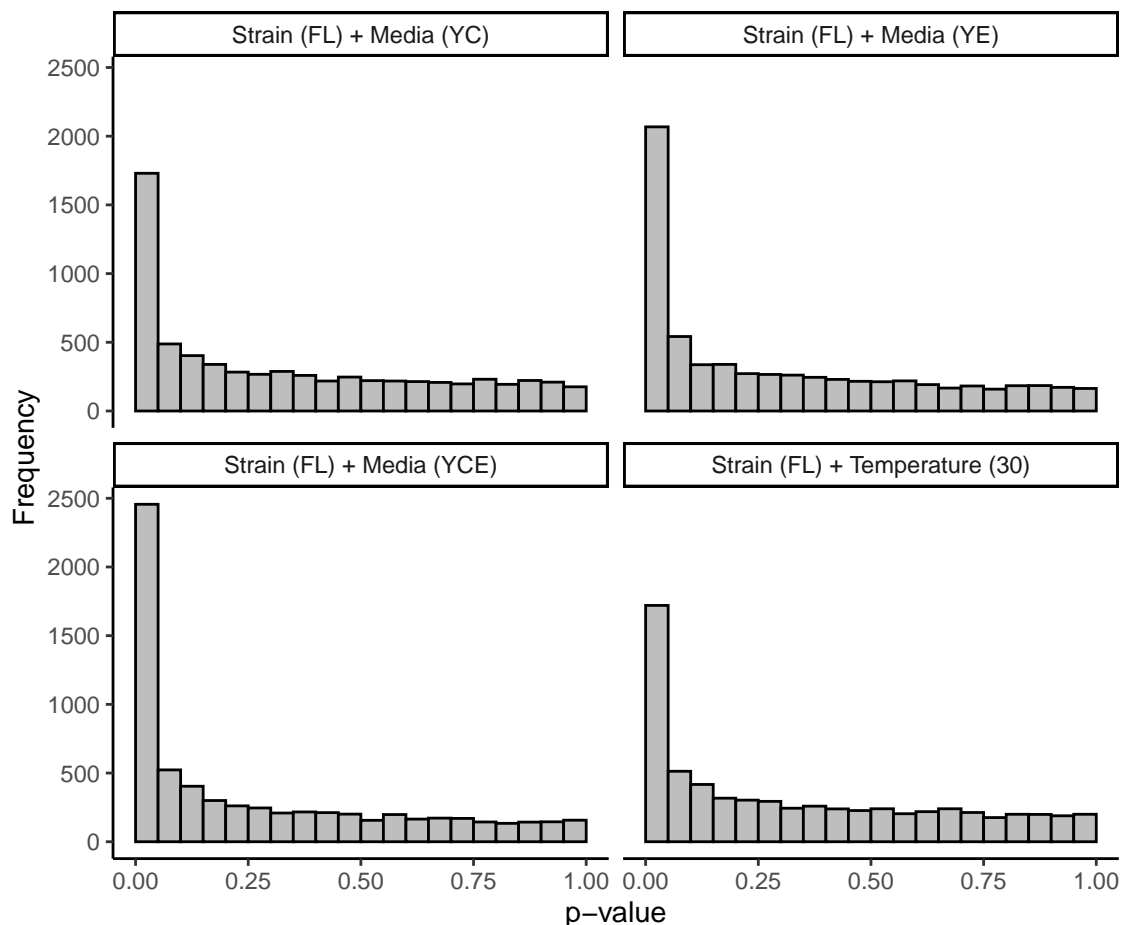


**Figure S4.7:** Histograms of unadjusted p-values for each contrast.

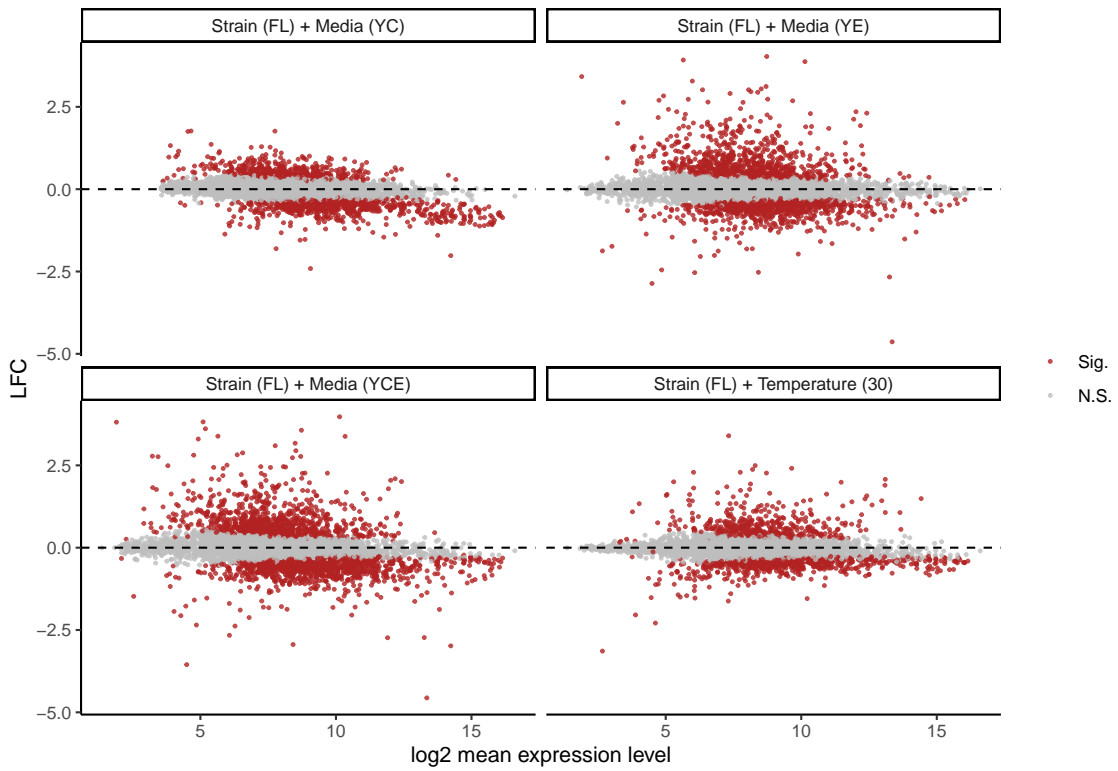


**Figure S4.8:** MA plots displaying log2 fold change (LFC) estimates with shrinkage across mean expression levels for each contrast. Red points indicate significantly differentially expressed genes, while gray points represent non-significant genes.

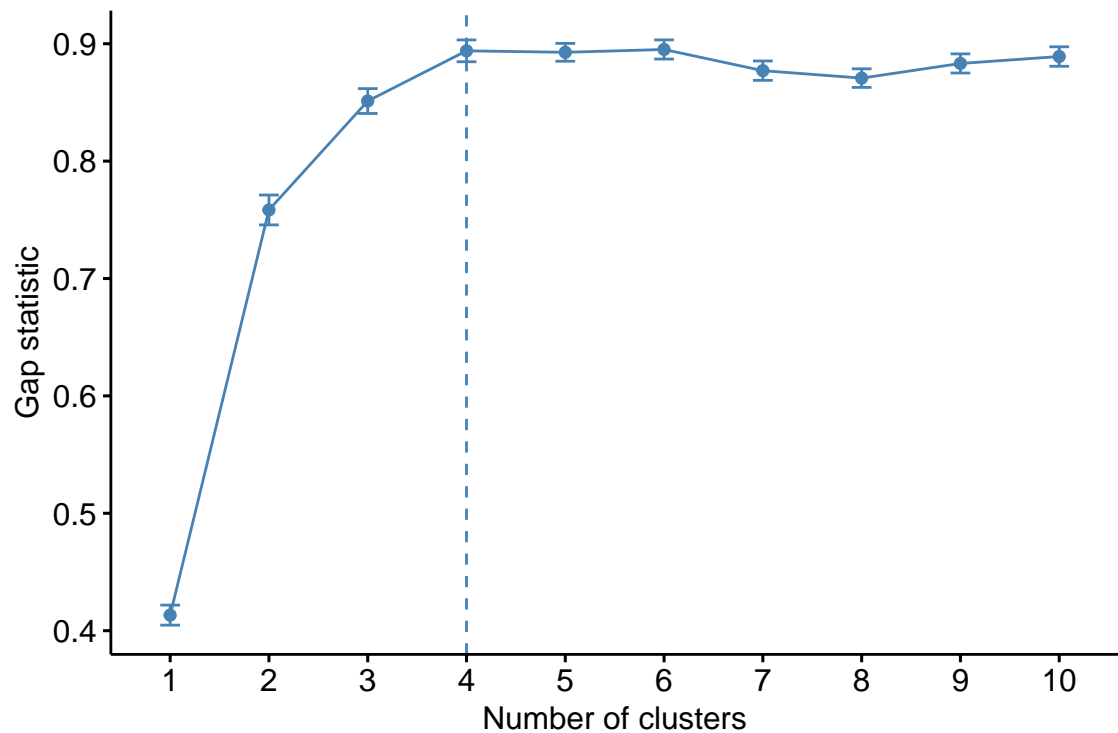


**Figure S4.9:** Gap statistic plot showing the optimal number of clusters for the top 500 most variable genes based on rlog-transformed data. The optimal cluster number is indicated by the vertical dashed line.